

We are IntechOpen, the world's leading publisher of Open Access books Built by scientists, for scientists

6,900

Open access books available

185,000

International authors and editors

200M

Downloads

Our authors are among the

154

Countries delivered to

TOP 1%

most cited scientists

12.2%

Contributors from top 500 universities



WEB OF SCIENCE™

Selection of our books indexed in the Book Citation Index
in Web of Science™ Core Collection (BKCI)

Interested in publishing with us?
Contact book.department@intechopen.com

Numbers displayed above are based on latest data collected.
For more information visit www.intechopen.com



Study of Adsorption Properties of Bentonite Clay

*Reda Marouf, Nacer Dali, Nadia Boudouara,
Fatima Ouadjenia and Faiza Zahaf*

Abstract

The clay used in this study was the bentonite from Mostagnem, Algeria. This material is used in many fields such as drilling, foundry, painting, ceramics, etc. It can also be applied in the treatment of wastewaters from chemical industries by means of adsorption. In this chapter the physicochemical properties of bentonite were determined by using several analyses techniques such as chemical composition, XRD, FTIR and S_{BET} . The bentonite was intercalated by aluminum polycations solution and cetyltrimethyl ammonium bromide. The acid activation of natural bentonite was performed by treatment with hydrochloric acid at different concentrations. The surface water pollutants removed by the modified bentonites are bemacid yellow E-4G and reactive MX-4R dyes, and fungicide chlorothalnil. The Langmuir and Freundlich adsorption models were applied to describe the related isotherms. The pseudo-first order and pseudo-second order kinetic models were used to describe the kinetic data. The changes of enthalpy, entropy and Gibbs free energy of adsorption process were also calculated.

Keywords: montmorillonite, bentonite, adsorption, dyes, fungicide

1. Introduction

Bentonite clay is a volcanic rock that was deposited as volcanic ash in fresh or salt water millions of years ago. It was first discovered in 1890 in Wyoming (Montana, USA) near the Fort Benton site, hence its name. Currently there are a large number of bentonite deposits in the world, in USA, in Europe, in North Africa, in Japan, in China ... In Algeria, the most economically important bentonite deposits are found in the west. We note in particular the quarry of Maghnia (Tlemcen) with reserves estimated at one million tons and that of M'zila (Mostaganem) with reserves of two million tons [1, 2].

Bentonite is very soft plastic clay composed mainly of montmorillonite, a clay mineral 2: 1 type of phyllosilicate family formed of fine particles. Montmorillonite consists of two tetrahedral layers (SiO_4) separated by an octahedral layer ($\text{Al}(\text{OH})_6$), its chemical formula is $(\text{Al}, \text{M}^{2+})_2 \text{Si}_4 \text{O}_{10} (\text{OH})_2, n \text{H}_2\text{O}$ with $\text{M}^{2+} = \text{Mg}, \text{Fe}, \dots$ (**Figure 1**) [3]. The total thickness of the sheet is approximately 14 Å. Montmorillonites has a negative charge on the surface, neutralized by compensating cations, the main origin of this surface charge comes from isomorphic substitutions resulting from the replacement of the metal cations of the lattice by cations of the same size but of lower charge (the substitution Al^{3+} by Mg^{2+} or Fe^{2+} and the substitution of Si^{4+} by Al^{3+}).

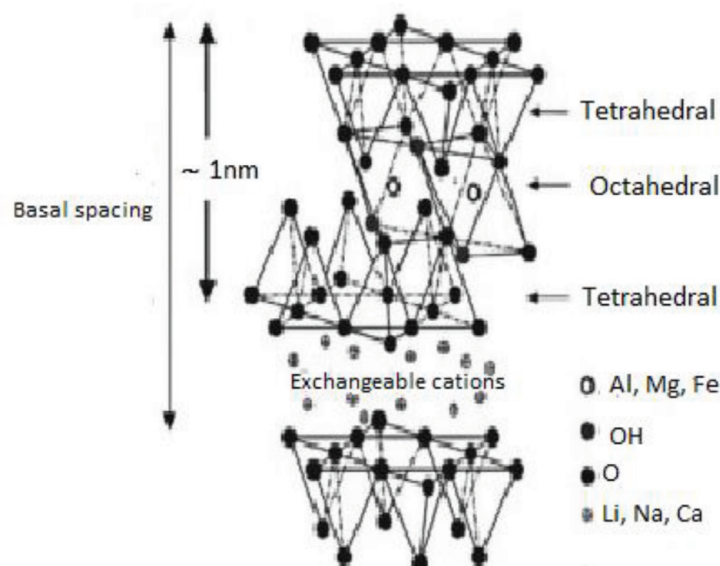


Figure 1.
Montmorillonite structure.

Bentonite has a privileged place in the purification of water [4, 5]. High specific surface area, chemical and mechanical stabilities, layered structure, high cation exchange capacity (CEC), tendency to hold water in the interlayer sites, and the presence of Brønsted and Lewis acidity have made clays excellent adsorbent materials [6, 7]. The chemical nature and pore structure of bentonite generally determine their adsorption ability [8, 9].

The adsorption properties of natural clay minerals can often be improved either by intercalation of organic, inorganic, or organometallic molecules in the interlayer space, or by heat or acid treatments [10, 11]. XRD measurements show that intercalation increases the spacing between layers. Among these modifications, the insertion of clays by poly cationic solutions has been used widely in recent years [12, 13]. In addition to their catalytic power, they are presented as excellent adsorbents. The main qualities that these pillared clays can develop are a high specific surface area and a large pore volume.

For the poly cation intercalation pillars to execute correctly, the synthesis protocol must pass through three steps: the first is to prepare the pillaring solution based on multivalent cation such as Al^{3+} , Fe^{3+} or Cr^{3+} . The second is the impregnation of the polycationic solution within the interlayer space [10, 14]. The last step is the calcination at temperature between 400 and 500 °C in order to solidify the pillars [15]. Some examples for montmorillonite intercalating by polycations cited in literature are the following: china montmorillonite was pillared by solution of Al_{13} polycations to eliminate cadmium [16], the bentonite of Turkish origin pillared with Fe and Cr was applied as adsorbent for carbon oxide (CO_2) and hydrogen H_2 [17], the Al/Ti and Al/Zr- pillared montmorillonites from Brazilian Amazon was used for zinc cation removal [18] and Fe/Zr-pillared montmorilointe (Guangdong, China) was tested for Cr(VI) removal [19].

The organic intercalation of montmorillonite can significantly enhance the organophilicity of the resultant product. Cationic organic compounds, such as surfactant cations, exchange the interlayer cations of montmorillonite [20], and the resulting organoclay is excellent for diverse organic pollutants, e.g. phenol [21], dye [22], and VOCs [23, 24]. Quaternary alkylammonium compounds (bromides or chlorides) are the most commonly employed for intercalation into bentonites. Due to their long-chain they offered to the clays a larger interlayer spacing. The most quaternary ammonium surfactants used are cethyltrimethyl ammonium bromide

(CTMAB), tetramethyl ammonium (TMA), trimethyl-phenyl ammonium (TMPA), dodecyl trimethyl ammonium and dimethyl sulfoxide (DMSO).

Unfortunately, sometimes the insertion of a surfactant weakens the specific surface of an organo-clay. To remedy this disadvantage, it's preferable to combine the intercalation of organic pillar with another mineral. For example, Jiang et al. used hexadecyltrimethyl ammonium bromide added to Al/Fe-pillared montmorillonite [25]. Zhu's group prepared an intercalated montmorillonite with both hexadecyltrimethyl ammonium bromide and Al¹³ cations, and discussed the influence of the addition sequence of these two modifiers on the final products [26].

Another method applied to improve adsorption capacity of bentonite consists of the reaction of clay minerals with a strong mineral acid solution, usually hydrochloric acid (HCl) or sulfuric acid (H₂SO₄). Acid activation leads to modification of Mt. with improved properties such as enhanced surface area, pore diameters, number of acid sites, and catalytic activities. The treatment of the naturally occurring and purified Mt. with hot mineral acid replaces exchangeable cations with H⁺ ions. Gradual leaching of Al³⁺ out of both tetrahedral and octahedral sites occurs, but the silicate groups remain largely intact [27, 28].

Dyes released into wastewaters of different industrial plants such as dye manufacturing, textile, paper and food, are toxic, not degradable and stable. The presence of these substances in the surface waters can be carcinogenic and causes damage to human beings, such as dysfunction of kidneys and central nervous system [29, 30].

Pesticides are synthesized substances or biological agents used for attracting any pest. They are mainly applied in agriculture to protect crops from insects, weeds, and bacterial or fungal diseases during growth [31]. Some pesticides, like fungicides are used to kill or inhibit growth of fungi or insects that parasitize crops [32]. Pesticides originating from human activity can also enter water bodies through surface runoff, leaching, and/or erosion. Pesticides can cause endocrine disruptions and neurological disturbances, influence immune system, reproduction and development [33].

Wastewaters containing dyes or pesticides are often treated by conventional methods as ozonation, membrane filtration, reverse osmosis, oxidation, ion exchange coagulation and adsorption [34–38]. Adsorption is considered as an attractive and favorable alternate for the removal of dyes and other organic molecules from wastewater streams. Many efforts have been made to find an appropriate adsorbent. Clay adsorbents enable to adsorb anionic and cationic pollutants such as dyes, pesticides and metal ions.

In this context, the present chapter focused in the application of Mostaganem bentonite in the treatment of natural water contaminated by dyes and pesticide. We will also study the phenomenon of adsorption of these pollutants through the use of mathematical models to determine the reaction mechanism, kinetics and thermodynamics of adsorption.

2. Materials and methods

Bentonite used in this investigation was purchased from M'zila deposit (Mostaganem, Algeria). This material is commercialized as industrial charge bentonite without additives by ENOF Company. The physicochemical properties of bentonite are resumed in chemical composition, point of zero charge, cation exchange capacity (CEC) and different analyses techniques such as XRD, FTIR, SEM and Specific surface area (BET).

The aim of the present study was the adsorption of two dyes, acid yellow E-4G and reactive yellow MX-4R. For this purpose two adsorbents were used: (i) bentonite intercalated by hydroxy-aluminum cations, (ii) bentonite pillared by cetyltrimethyl ammonium cation.

Bemacid Yellow E 4G (C.I. acid Yellow 49) and reactive Procion Yellow MX 4R (C.I. Reactive Yellow 14) were supplied by SOITEX textile society (Tlemcen, Algeria). The chemical formula and molecular weight of E-4G and MX-4R are $C_{16}H_{13}Cl_{12}N_5O_3S$; 426.24 g/mol and $C_{20}H_{19}ClN_4Na_2O_{11}S_3$; 669.02 g/mol, respectively. A stock solution (1.0 g/L) of dye was prepared by dissolving accurate weight amount in deionized water and the other concentrations were obtained by dilution of this stock dye solution.

The product chlorothalonil (Chl) fungicide was removed by acid activated bentonite from aqueous solution. Chl was obtained by Syngenta Protection of Plants S.A, Bale, Switzerland. It contains 400 g/L of chlorothalonil in the form of concentrated suspension with some impurities. The Chl is an inhibitor of spore germination, which acts on various enzymes and on the metabolism of fungi. The chemical formula of Chl is $C_8Cl_4N_2$, and its molecular weight is 265.93 g/mol. The solubility of chlorothalonil in water is 0.6 mg/L at 20 °C.

2.1 Preparation of pillared bentonite

The Al(III)-modified bentonite was obtained by mixing $AlCl_3$ solution (0.2 mol/L) with sodium hydroxide solution (0.2 mol/L) at 60 °C, up to the molar ratio $OH^-/Al^{3+} = 2$ [39]. The solution was aged at room temperature for three days before using. The resulting pillaring solution was added to the bentonite by stirring for 4 h at 70 °C at the ratio of 50 mmol oligomeric cations per gram of bentonite [40]. The slurry was stirred for 24 h at room temperature, filtered, and washed repeatedly with deionized water. The solid was dried at 80 °C and kept in a sealed bottle. The pillared bentonite obtained was designated as B-Al.

2.2 Preparation of CTAB-intercalated bentonite

The surfactant CTAB intercalated bentonite was synthesized as follows: the amount of CTAB (175 mg) corresponding to 1.0 times CEC of bentonite was dissolved in 1 L of distilled water at ambient temperature and stirred for 24 h. A total of 1 g bentonite was added to 100 mL surfactant solution. The dispersion was stirred for 4 h at 60 °C. The separated sample was washed several times and dried at 80 °C. The final product was noted as B-CTAB.

2.3 Acid activation of bentonite

Raw bentonite was treated by hydrochloric acid (HCl) (37% purity, Merck) at different concentrations (0.1, 1 and 6 N) at 70 °C. The amounts of 4 g of each treated sample were added to 400 mL of acid solution [41]. The contact time of the samples with the acid solution was fixed as 4 hours. At the end of treatment, the bentonite was washed several times with distilled water and dried over night at 80 °C [42].

2.4 Adsorption experiment

The adsorption experiments were carried out in a series of Erlenmeyer flasks containing 0.1 g of B-Al or B-CTAB and 20 mL of dyes aqueous solution at the desired concentration and initial pH (adjusted with hydrochloric acid 0.1 N or

0.1 N NaOH) in ambient temperature bath (23 °C). After shaking for 3 h of contact time, the flasks were removed and the concentration of MX-4R and E-4G after the adsorption was analyzed by spectrophotometer at wavelength of 425 and 400 nm, respectively. The adsorbed amount of dye (mg/g) was calculated as follow:

$$q_e = (C_0 - C_e) \cdot \frac{V}{m} \quad (1)$$

where, q_e (mg/g) is the equilibrium adsorption capacity, C_0 the initial dye concentration, C_e the equilibrium dye concentration (mg/L), V the volume of solution (L) m is the mass of the adsorbent (g).

The chlorothalonil was prepared in the range of initial concentrations 100–500 mg/L, in order to know the maximum amount of fungicide that bentonite can adsorb. For each experiment, 20 mL of pesticide solution was added to 0.1 g of the solid. The suspension was shaken at room temperature (23 °C) for 3 h. The chlorothalonil was detected by spectrophotometer at wavelength of 360 nm.

3. Results and discussions

3.1 Characterization of raw and modified bentonite

The chemical analysis of raw bentonite was performed by X-fluorescence XRF 9900. Thermo Instrument. The result of this analysis revealed that the silica (64.22%), alumina (11.62%) and lime (9.33%) are the main oxides of the bentonite with the existence of the others oxides in the small amounts such as Fe_2O_3 (4.88%), TiO_2 (1.06%), Na_2O (3.38%) and P_2O_5 (0.03%). The elementary analysis of M'zila bentonite gives the formula $\text{Na}_{0.13} \text{Ca}_{0.01} \text{K}_{0.10} (\text{Al}_{1.24} \text{Mg}_{0.2} \text{Fe}_{0.17} \text{Ti}_{0.01}) (\text{Si}_{4.24}) \text{O}_{10} (\text{OH})_2$ with mass molar 368.68 g/mol [43].

The pH_{PZC} value purified bentonite was found as 6.8. This value informs us about the electric charge on the solid surface. At pH value below than pH_{PZC} the electrical charge on the surface is positive, it will be negative at pH higher than pH_{PZC} . Cation exchange capacity of natural bentonite was determined to be 112 meq/100 g by applying the conductimetric titration method [44]. The BET specific surface area measured via Quantachrome instrument was found 59.02 m^2/g .

The diffractogram of raw bentonite was shown in **Figure 2**. The bentonite sample contains some mineral phases such as the Montmorillonite (M), Kaolinite (K), Calcite (C), Quartz (Q) and Dolomite (D). The characteristic peak d_{001} of montmorillonite appears at $2\theta = 5.5^\circ$, the kaolinite is observed at $2\theta = 10^\circ$ and the peak of calcite appears at $2\theta = 31^\circ$.

The FT-IR spectrum of raw bentonite was performed with Agilent Cary 630 Spectrometer in range of 4000–400 cm^{-1} . The FT-IR analysis illustrated in **Figure 3** shows an intensive band at 1000 cm^{-1} which is attributed to the Si-O in plan stretching vibration and other bands at 520 and 470 cm^{-1} assigned to Al-O-Si (octahedral Al) and Si-O-Si bending vibrations, respectively [45]. The small band at 1620 cm^{-1} is attributed to the deformation vibrations of the O-H bond of the constitution water. The band at 3620 cm^{-1} is assigned to hydroxyl groups Al^{3+} is partially replaced by Fe^{3+} and Mg^{2+} .

The images of scanning electron microscope were made by microscope JSM-6360 to observe the morphology of bentonite particles. According to the **Figure 4** the particles were formed by heterogeneous aggregates of different shape and size. It appears that these grains constitute a stack of sheets probably representing the

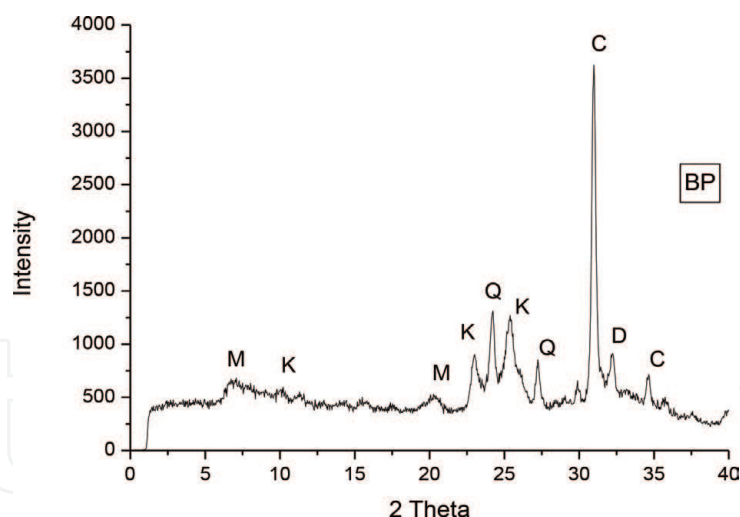


Figure 2.
XRD pattern of raw bentonite.

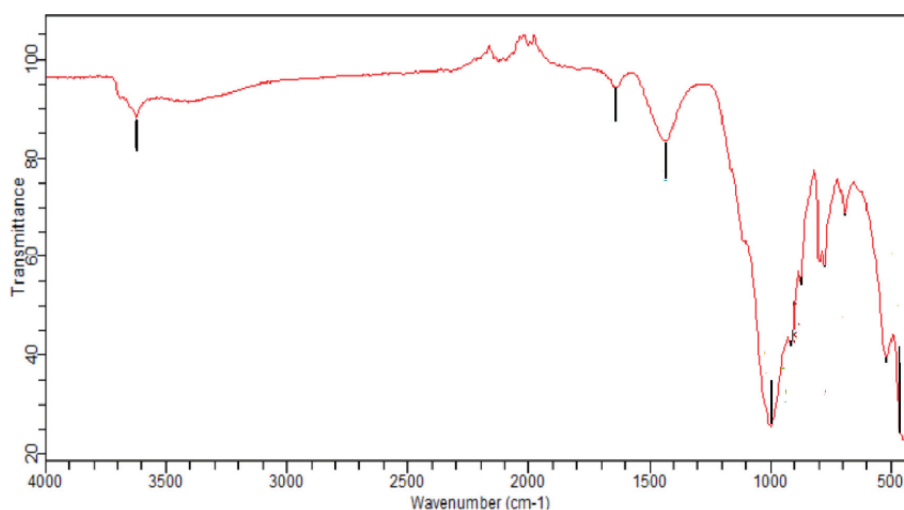


Figure 3.
FT-IR spectra of raw bentonite.

clay layers. On the surface of the sample, a small luminous crystallite settles, may be of free silica (quartz).

According to the XRD analysis realized with INEL CPS 120 instrument employing cobalt radiation ($\lambda = 0.178$ nm), the hydroxy-aluminum polycations exchange increases the d_{001} value to 14.3 Å, but the peak was much less intense compared to that of natural bentonite (**Figure 5**). The reduction in diffractogram might be caused by collapsing of the Mt. layers due to partial incongruent phase transition of hydroxy-Al into Fe/Al oxides and their interactions during aging and drying, as suggested by Thomas et al. [46].

The addition of surfactant causes the increasing of basal spacing of the bentonite around 18 Å, indicating location of CTA⁺ ions between layers of montmorillonite. In order to increase more again the basal spacing, it must be increase in CTA⁺ concentration, because as known, the amount of added surfactant has a direct effect on the interlayer expansion of Mt.

The pillaring bentonite with hydroxy-aluminum and CATB generated an enhancement of specific surface area where the values found were 110 and 194.4 m²/g for B-Al and B-CTAB, respectively. These values were very higher than that of untreated bentonite (59.02 m²/g). In the case of Al-modified bentonite the specific surface area was increased significantly but a slight increase was noted

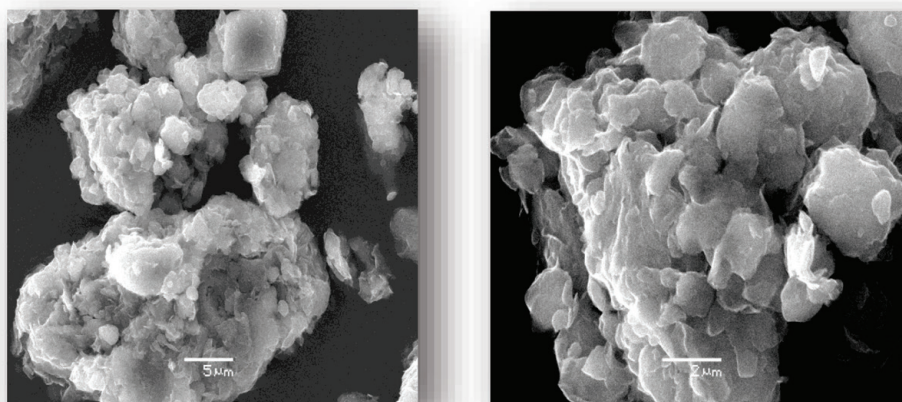


Figure 4.
SEM images of natural bentonite extension 3000 and 9000.

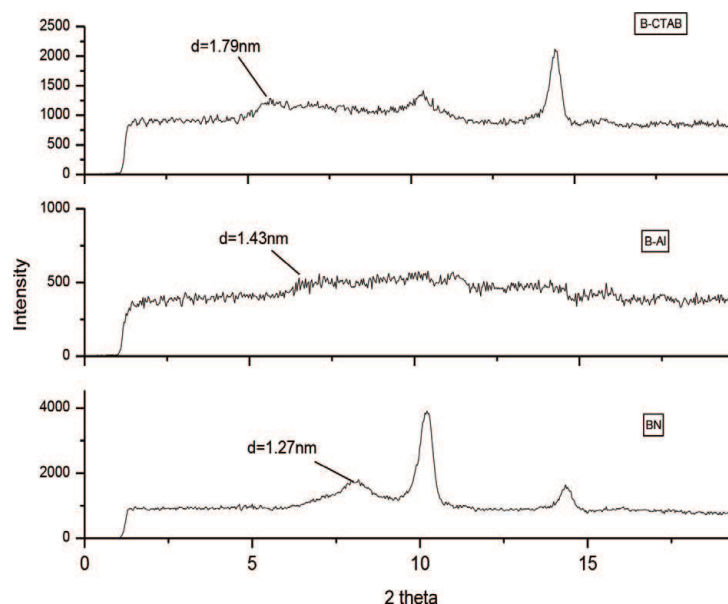


Figure 5.
XRD patterns of natural and pillared bentonite.

through the basal spacing. This is due to the existence of electrostatic bonding between the negatively charged layers and pillaring oligocations in uncalcined Al-pillared clay.

The second application deals with the acid activation of Algerian bentonite and testing of its capacity to remove the chlorothalonil fungicide in aqueous solution. The hydrochloric acid solutions were used in the concentration range of 0.1-6 N.

The specific surface area of bentonite treated by 1 N (BA1N) and 6 N (BA 6 N) of hydrochloric acid were determined as 82.22 and 80.55 m²/g, respectively. We see that the specific surface areas of both activated bentonites are almost identical, which are much higher than that of the raw bentonite (59.02 m²/g). The specific surface area greatly increases at the acid concentration of 1 N, but slightly decreases at the concentrations higher than this value and then does not change much. Similar results were found by activating bentonite with sulfuric acid [47, 48].

The XRD patterns of raw and activated bentonites at various concentrations (0.1, 1 and 6 N) were shown in **Figure 6**. We note that there is no difference between the spectra of BN and BA 0.1 N. The concentration of 0.1 N of hydrochloric solution seems not be sufficient to make significant changes in the structure of

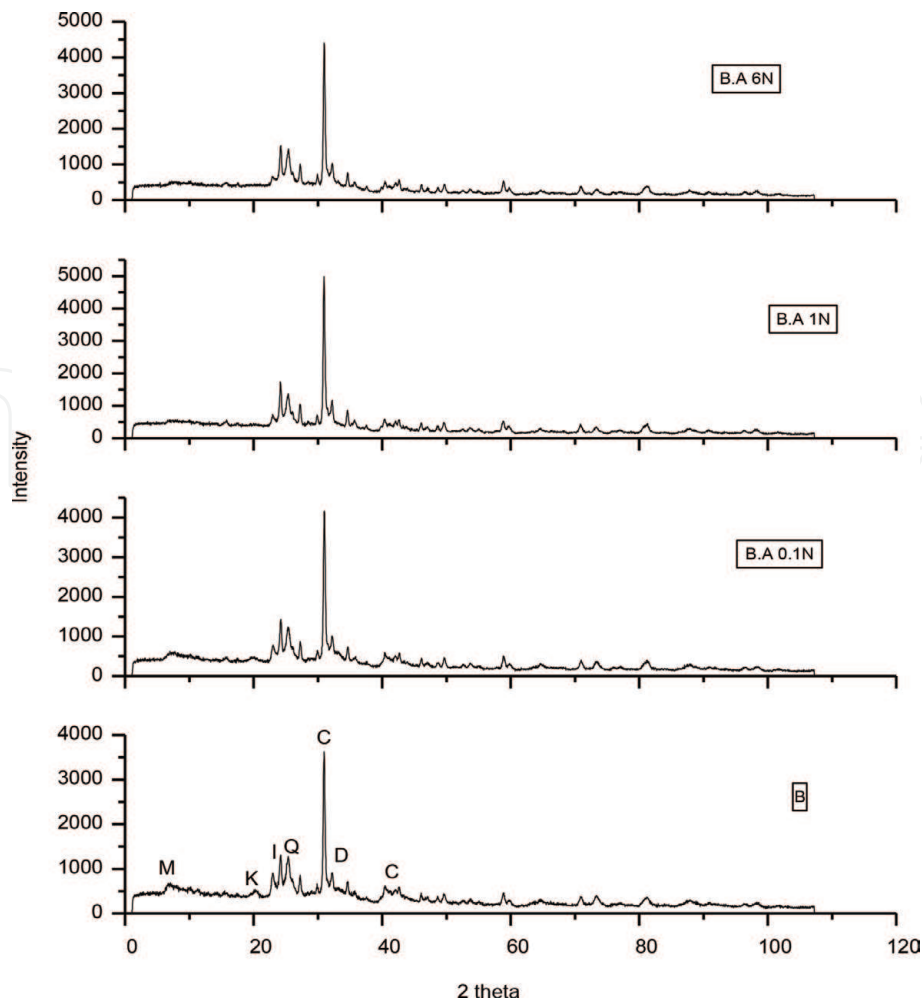


Figure 6.
XRD patterns of raw and activated bentonites.

bentonite. This means that it is a cation exchange causing the substitution of the exchangeable cations of interlayer space by protons H^+ . In contrast to the sample treated with 0.1 N, the samples BA 1 N and BA 6 N undergo a significant structural modification according to the XRD spectra, where we notice that the peaks of montmorillonite and the kaolinite almost disappeared, while that of the illite is reduced in intensity. So from 1 N concentration of HCl, the clay minerals of bentonite are exposed to the direct effect of acid leading to the destruction of the basic clay sheets.

This process generally increases the surface area and the acidity of the clay minerals [49].

3.2 Adsorption isotherms of dyes and models fitting

The adsorption isotherms are realized at different initial concentrations of dyes, adsorbent dose was 5 g/L, and pH effect was tested and maximum adsorbed amount of dye was noted at $pH = 2-3$. The isotherms are formed by amount of dye adsorbed by the plot vs. equilibrium concentration. The adsorption isotherms of MX-4R and E-4G by the pillared bentonites are presented in **Figure 7**. The results show that the amount of dye adsorbed increases with the increase in equilibrium concentration of dye. All isotherms are of S-shape according to the classification of Giles et al. [50]. This type of isotherm originates from the cooperative isothermal adsorption, i.e. the adsorbed molecules promote higher adsorption of other molecules and tend to be adsorbed in groups. The maximum adsorbed amounts registered were 93.91 and

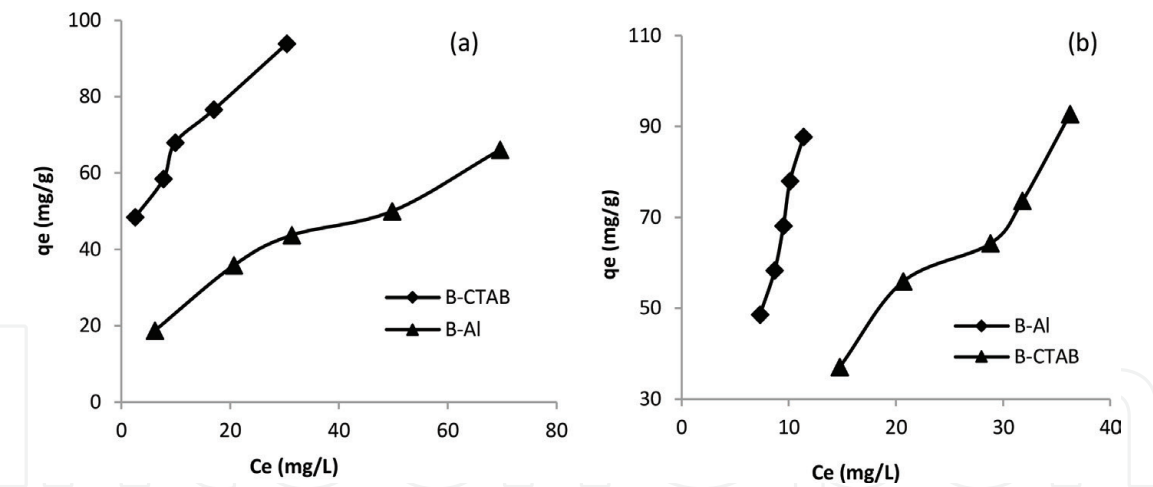


Figure 7. Adsorption isotherms of (a) MX-4R and (b) E-4G onto B-Al and B-CTAB. ($C_0 = 200\text{--}500\text{ mg/L}$, $pH = 2\text{--}3$, adsorbent dose 5 g/L , contact time 3 h)

92.75 mg/g for MX-4R and E-4G respectively, attributed to B-CTAB sample. Those of B-Al adsorbent were 66.08 and 87.72 mg/g, respectively. According to these results, the B-CTAB sample has adsorption capacity most important than that of B-Al for the both dyes, in same operating conditions.

The adsorption isotherms were fitted by Langmuir and Freundlich equations expressed in linear forms in relations (2) and (3), respectively:

$$\frac{C_e}{q_e} = \frac{C_e}{Q_0} + \frac{1}{K_L Q_0} \tag{2}$$

where Q_0 is the maximum adsorption capacity (mg/g), and K_L (L/mg) is a constant that relates to the heat of adsorption.

$$\log q_e = \log K_F + \frac{1}{n} \log C_e \tag{3}$$

K_F and n are the Freundlich constants, indicating the capacity and intensity of adsorption, respectively.

The Langmuir and Freundlich constants and the linear regression correlations (R^2) for both isotherms model are listed in **Table 1**. The results reveal that the adsorption isotherms correlate with Freundlich model because the correlation coefficient (R^2) values obtained were above 0.98, while the model of Langmuir describes less well the experimental data where the linearization constants were insignificant except in the case of MX-4R. However Freundlich model is well used to describe the adsorption behavior of dyes on the both materials. This can be explained by the fact that the Langmuir equation is valid for monolayer adsorption onto a surface containing a finite number of identical sites, while Freundlich isotherm represents satisfactorily the sorption data on heterogeneous surfaces.

3.3 Adsorption kinetics of dyes

To evaluate the adsorption rate, the adsorption kinetic was examined by pseudo-first order and pseudo-second order models. The evolution of adsorption capacity of MX-4R and E-4G dyes increases over time and attained an equilibrium state around 60 min. The adsorption rates of the E-4G and MX-4R by intercalated bentonites are rapid early in the process and becoming slower over time. The

Model		Langmuir			Freundlich		
Constants		Q ₀ (mg/g)	K _L (L/mg)	R ²	1/n	K _F mg/g(L/mg) ^{1/n}	R ²
B-Al	E-4G	ins	ins	ins	1.396	2.96	0.984
	MX-4R	76.92	0.044	0.989	0.455	8.60	0.988
B-CTAB	E-4G	ins	ins	ins	0.920	3.177	0.955
	MX-4R	113.63	0.137	0.994	0.346	28.73	0.984

ins: insignificant results.

Table 1.
Linearization constants of Langmuir and Freundlich equations.

pseudo-first order kinetic using the linear Lagergren equation is generally expressed as follows [51]:

$$\ln(q_e - q_t) = \ln q_e - k_1 t \tag{4}$$

where q_t is amount adsorbed of dye at time t (mg/g) and k_1 is the rate constant of the pseudo-first order model (min^{-1}). The k_1 and q_e were calculated from the slope and intercept of plots $\ln(q_e - q_t)$ versus t , respectively.

The pseudo-second order kinetic is expressed as follows [52]:

$$\frac{t}{q_t} = \frac{1}{k_2 q_e^2} + \frac{t}{q_e} \tag{5}$$

where k_2 is the rate constant of the pseudo-second order model for the adsorption process (g/mg.min). Plots of t/q_t against t have been drawn to obtain the rate parameters.

The calculated q_e values agree with the experimental q_e values, and the correlation coefficients for the pseudo-second-order kinetic plots were also found to be very high ($R^2 = 0.98$), indicating that pseudo-second order model fitted very well the kinetic adsorption. The pseudo second order model is based on the assumption that the rate limiting step may be chemisorption which involves valence forces by sharing or electron exchange between the adsorbent and the adsorbate [53]. According to the **Table 2**, the rate constants increase from 0.002 and 0.011 $\text{g.mg}^{-1} \text{min}^{-1}$ (B-CTAB) to 0.922 and 0.912 $\text{g.mg}^{-1} \text{min}^{-1}$ (B-Al). This means that the adsorption of dyes onto B-Al is a fast reaction, and CTAB-modified bentonite has a best adsorption capacity due to its high porosity and its large specific surface area.

3.4 Adsorption isotherms of chlorothalonil

The **Figure 8** shows the adsorption of Chl by the activated bentonite. This figure indicates that the adsorbed amount of Chl onto raw and activated bentonite increases in parallel with the equilibrium concentration. The experimental isotherm obtained here may be classified as type S referring to the classification of Giles et al. This type of isotherm originates from the cooperative isothermal adsorption, i.e. the adsorbed molecules promote higher adsorption of other molecules and tend to be adsorbed in groups. We note also that the activated bentonite adsorbs much better than the natural bentonite. When the activated

Model	B-Al		B-CTAB	
	E-4G	MX-4R	E-4G	MX-4R
Pseudo-first order				
$q_{e(cal)}$ (mg/g)	0.835	19.36	35.70	3.010
K_1 (min^{-1})	0.019	0.065	0.043	0.019
R^2	0.809	0.902	0.970	0.350
Pseudo-second order				
$q_{e(cal)}$ (mg/g)	12.048	45.455	42.016	60.24
K_2 (g/mg.min)	0.922	0.912	0.002	0.011
R^2	0.999	0.997	0.996	0.999
$q_{e(exp)}$ (mg/g)	11.865	44.207	38.926	59.588

Table 2.
Constants rates of the E-4G and MX-4R adsorption by B-Al and B-CTAB.

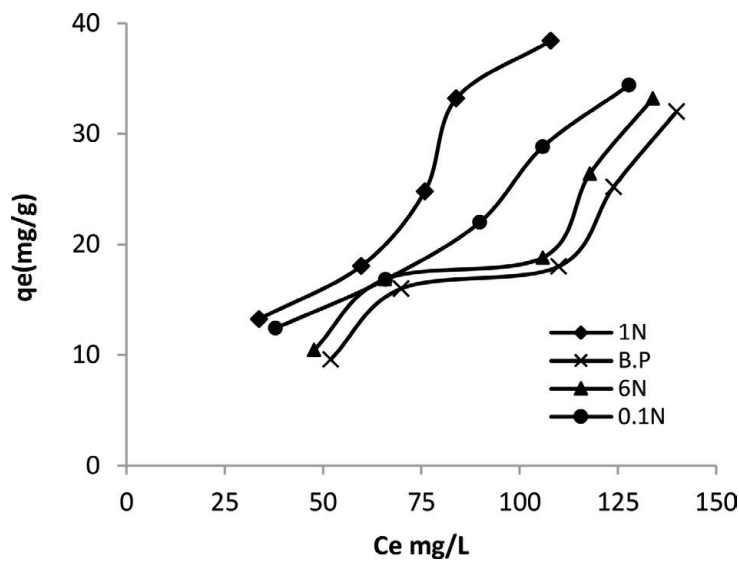


Figure 8.
Adsorption isotherms of Chl onto activated bentonite.

Sample	T (K)	K_F (mg/g (L/mg) ^{1/n})	1/n	R^2
BA 0.1 N	296	0.913	0.737	0.935
BA 1 N	296	0.590	0.939	0.925
	303	2.064	0.725	0.950
	313	2.295	0.831	0.979
	323	2.087	0.736	0.970

Table 3.
The constants of Freundlich model.

samples were compared, it was found that the maximum amount of adsorption (38.42 mg/g) was observed for BA 1 N.
The isotherm model fit the experimental data very well is Freundlich model. The Freundlich equation is an empirical equation that can be used for

heterogeneous systems with interaction between the molecules adsorbed. As seen from **Table 3**, the values of regression coefficients R^2 were close to the unit and the $1/n$ values were less than unity which indicates that the adsorption intensity was favorable and was a physical process. On the other hand, the experimental data fitted by Langmuir model were insignificant in terms of adsorption; this is why they are not mentioned.

3.5 Adsorption heats of chlorothalonil

In the case of adsorption of molecules on a solid surface, the Gibbs energy is composed of two functions, the enthalpy function (H), which is measure of the energy of interaction between the molecules and the adsorbent surface, and the entropy function (S), which reflects the change and the arrangement of molecules in the liquid phase and on the surface. The free energy ΔG was calculated according the following relation:

$$\Delta G^0 = \Delta H^0 - T \Delta S^0 \tag{6}$$

The distribution coefficient K_d (L/g) is calculated from the following Equations [54, 55]:

$$\ln K_d = \frac{\Delta S^0}{R} - \frac{\Delta H^0}{RT} \tag{7}$$

$$K_d = \frac{(C_0 - C_e)}{C_e} \cdot \frac{V}{m} \tag{8}$$

where ΔH^0 , ΔS^0 , and T are the adsorption enthalpy (kJ/mol), entropy (J/mol.K) and temperature in Kelvin, respectively, and R is the gas constant (8.31 J/mol.K). The slope and intercept of the plot of $\ln K_d$ versus $1/T$ correspond to $\Delta H^0/R$ and $\Delta S^0/R$, respectively.

It can be seen from **Table 4** that the calculated ΔG^0 values have negative signs, indicating that the adsorption process is spontaneous in the experimental conditions and the spontaneity increases with increasing of temperature. All enthalpy values are positive, showing that the adsorption process is endothermic. The magnitude of enthalpy values suggests that the adsorption of Chl onto activated bentonite was physic in nature. The entropy values were positive that means the molecules disorder was located in interface solution/solid.

		C ₀ (mg/L)	ΔH° (kJ/mol)	ΔS° (J/molK)	ΔG° (kJ/mol)			
					303 K	313 K	323 K	R ²
BA 1 N	30	68.894	234.292	- 2.096	- 4.439	- 6.782	0.930	
	40	34.020	120.528	- 2.499	- 3.705	- 4.910	0.895	
	50	29.726	107.381	- 2.810	- 3.883	- 4.957	0.927	
	60	39.861	137.879	- 1.915	- 3.294	- 4.673	0.926	
	80	40.422	141.319	- 2.397	- 3.810	- 5.223	0.910	

Table 4.
Heats adsorption of Chl onto activated bentonite.

4. Conclusions

In this research we studied the characteristics and the physicochemical properties of an Algerian bentonite which its adsorption capacity was tested to eliminate organic pollutants from aqueous solution.

Before the adsorption experiment, bentonite underwent two different treatments in order to improve its exchange capacity and porosity. The first treatment carried out is that of the pillaring clay with mineral (polycations of Al_{13}) and organic (CTAMB) intercalants. The second is the treatment by acid attack (HCl) at different concentrations (0.1, 1 and 6 N).

The intercalation of the bentonite by Al_{13} and CTAB increased the basal sheet space up to 14.3 and 18 Å, respectively. The chemical activation with HCl at 6 N concentration enhanced the specific surface area of the bentonite from 59.02 to a value of 82 m²/g. The obtained materials from the both treatments were applied for the adsorption of MX-4R, E-4G dyes and the fungicide chlorothalonil.

The adsorption isotherms of these pollutants have shown that the adsorption capacities were very satisfactory and the adsorption phenomenon was physical nature. The adsorption isotherms of all adsorbates were well described by Freundlich model. Kinetic data of dyes adsorption tend to fit well in pseudo-second order rate expression. Moreover the adsorption of chlorothalonil by activated bentonite was spontaneous and this spontaneity increases with increasing temperature.

Conflict of interest

The authors declare no conflict of interest in publishing this chapter.

Author details

Reda Marouf*, Nacer Dali, Nadia Boudouara, Fatima Ouadjenia and Faiza Zahaf
Faculty of Exacts Sciences, Laboratory of Materials, Applications and Environment,
University Mustapha Stambouli of Mascara, Algeria

*Address all correspondence to: r.marouf@univ-mascara.dz

IntechOpen

© 2021 The Author(s). Licensee IntechOpen. This chapter is distributed under the terms of the Creative Commons Attribution License (<http://creativecommons.org/licenses/by/3.0>), which permits unrestricted use, distribution, and reproduction in any medium, provided the original work is properly cited. 

References

- [1] Achour S, Youcef L, élimination du cadmium par adsorption sur bentonites sodique et calcique (Cadmium removal by adsorption on sodic and calcic bentonites) . Larhyss Journal. 2003;2:69-81.
- [2] Youcef L, Achour S, Etude de l'élimination des fluorures des eaux de boisson par adsorption sur bentonite (Removal study of fluorides from drinking wtaers by adsorption on bentonite). Larhyss Journal. 2004; 3:129-142.
- [3] Suquet H, de la Calle C, Pezerat H, Swelling and structural organization of saponite. Clay Clay Miner. 1975;23: 1-9. DOI: 10.1346/CCMN.1975.0230101
- [4] Arfaoui, S, Frini-Srasra N, Srasra E, Application of clays to treatment of tannery sewages. Desalination. 2005; 185 :419-426. DOI: 10.1016/j.desal.2005.04.047
- [5] Hamdi, N, Srasra E, Remove of fluoride from acidic wastewater by clay mineral effect of solid–liquid ratios. Desalination. 2007; 206:238-244. DOI: 10.1016/j.desal.2006.04.054
- [6] Al-Asheh S, Banat F, Abu-Aitah L, Adsorption of phenol using different types of activated bentonites. Sep. Purif. Technol. 2003; 33: 1-10. DOI : 10.1016/S1383-5866(02)00180-6
- [7] Fu-Chuang H, Jiunn-Fwu L, Chung-Kung L, Huang-Ping C, Effects of cation exchange on the pore and surface structure and adsorption characteristics of montmorillonite. Colloid Surf. A: Physicochem. Eng. Aspects. 2004; 239: 41-47. DOI: 10.1016/j.colsurfa.2003.10.030
- [8] Min-Yu T, Su-Hsia L, Removal of basic dye from water onto pristine and HCl activated montmorillonite in fixed beds. Desalination. 2006;194: 156-165. DOI : 10.1016/j.desal.2005.11.008
- [9] Okada, K, Arimitsu N, Kameshima Y, Akira N, Kenneth MacKenzie JD, Solid acidity of 2:1 type clay minerals activated by selective leaching. Appl. Clay Sci. 2006;31: 185-193. DOI: 10.1016/j.clay.2005.10.014
- [10] Pinnavaia TJ, Intercalated clay catalysts. Science. 1983;220: 365-371. DOI: 10.1126/science.220.4595.365
- [11] Carrado KA, Synthetic organo- and polymer-clays: preparation, characterization, and materials applications. Appl. Clay Sci. 2000;17: 1-23. DOI: 10.1016/S0169-1317(00)00005-3
- [12] A. Vaccari, Preparation and catalytic properties of cationic and anionic clays. Catal. Today. 1998;41: 53-71. DOI: 10.1016/S0920-5861(98)00038-8
- [13] Hernando MJ, Pesquera C, Blanco C, Gonzalez F, Comparative study of the texture of montmorillonites pillared with aluminum and aluminum/cerium. Langmui. 2001;17 : 5156-5159. DOI: 10.1021/la010157k
- [14] Ding Z, Klopprogge JT, Frost RL, Porous clays and pillared clays-based catalysts. Part 2: a review of the catalytic and molecular sieve applications. J. Porous Mater. 2001;8: 273-293. DOI: 10.1023/A:1013113030912
- [15] Gil A, Korili SA, Trujillano R, Vicente MA, A review on characterization of pillared clays by specific techniques. Appl. Clay Sci. 2011;53: 97-105. DOI: 10.1016/j.clay.2010.09.018
- [16] Yan LG, Shan X-Q, Adsorption of cadmium onto Al₁₃-pillared acid-activated montmorillonite. J. Hazard. Mater. 2008;156: 499-508. DOI: 10.1016/j.jhazmat.2007.12.045
- [17] Tomul F, Adsorption and catalytic properties of Fe/Cr-pillared bentonites.

Chem. Eng. J. 2012;185-186: 380-390.
DOI/ 10.1016/j.cej.2012.01.094

[18] Guerra DL, Airoidi C., Lemos VP, Angélica RS, Adsorptive, thermodynamic and kinetic performances of Al/Ti and Al/Zr-pillared clays from the Brazilian Amazon region for zinc cation removal. J. Hazard. Mater. 2008;155: 230-242. DOI: 10.1016/j.jhazmat.2007.11.054

[19] Zhou J, Wu P, Dang Z, Zhu N, Li P, Wu J, Wang X, Polymeric Fe/Zr pillared montmorillonite for the removal of Cr(VI) from aqueous solutions. Chem. Eng. J. 2010;162: 1035-1044. DOI: 10.1016/j.cej.2010.07.016

[20] de Paiva LB, Morales AR, Diaz FRV, Organoclays: properties, preparation and applications. Appl. Clay Sci. 2008 ;42(1-2): 8-24. DOI: 10.1016/j.clay.2008.02.006

[21] Zhou Q, He HP, Zhu JX, Shen W, Frost RL, Yuan P, Mechanism of p-nitrophenol adsorption from aqueous solution by HDTMA⁺ pillared montmorillonite-implications for water purification. J. Hazard. Mater. 2008.;154(1-3): 1025-1032. DOI: 10.1016/j.jhazmat.2007.11.009

[22] Ozcan A, Omeroglu C, Erdogan Y, Ozcan AS, Modification of bentonite with a cationic surfactant: an adsorption study of textile dye Reactive Blue 19. J. Hazard. Mater. 2007;140(1-2): 173-179. DOI: 10.1016/j.jhazmat.2006.06.138

[23] Jarraya I, Fourmentin S, Benzina M, Bouaziz S, VOC adsorption on raw and modified clay materials. Chem. Geol. 2010;275 (1-2): 1-8. DOI: 10.1016/j.chemgeo.2010.04.004

[24] Park SJ, Kim YB, Yeo SD, Vapor adsorption of volatile organic compounds using organically modified clay. Sep. Sci. Technol. 2008; 43(5): 1174-1190. DOI: 10.1080/01496390801910138

[25] Jiang JQ, Cooper C, Ouki S, Comparison of modified montmorillonite adsorbents-part I: preparation, characterization and phenol adsorption. Chemosphere. 2002;47(7): 711-716. DOI: 10.1016/S0045-6535(02)00011-5

[26] Zhu LZ, Zhu RL, Simultaneous sorption of organic compounds and phosphate to inorganic-organic bentonites from water. Sep. Purif. Technol. 2007.;54 (1): 71-76. DOI: 10.1016/j.seppur.2006.08.009

[27] Falaras P, Kovanis I, Lezou F, Seiragakis G, Cottonseed oil bleaching by acid activated montmorillonite. Clays Clay Miner. 1999;34: 221-232. DOI: 10.1180/000985599546181

[28] Hussin F, Aroua MK., Daud WMAW,. Textural characteristics, surface chemistry and activation of bleaching earth: a review. Chem. Eng. J. 2011;170: 90-106. DOI: 10.1016/j.cej.2011.03.065

[29] Oyewo OA, Elemike EE, Onwudiwe DC, Onyango MS, Metal oxide-cellulose nanocomposites for the removal of toxic metals and dyes from wastewater. Int. J. Biol. Macromol. 2020;164:2477-2496. DOI: 10.1016/j.ijbiomac.2020.08.074

[30] Kaemkit C, Monvisade P, Siriphannon P, Nukeaw J, Water soluble chitosan intercalated montmorillonite nanocomposites for removal of Basic Blue 66 and Basic Yellow 1 from aqueous solution. J. Appl. Polym. Sci. 2013;128(1): 879-887. DOI: 10.1002/app.38255

[31] Bolognesi C, Merlo FD, Pesticides: human health effects. In: Nriagu JO, editor. Encyclopedia of environmental health. Burlington: Elsevier; 2011. 438-453 pp. DOI: 10.1016/b978-0-444-52272-6.00592-4

[32] Gupta PK, Herbicides and fungicides. In: Gupta RC, editor.

Reproductive and developmental toxicology. Amsterdam: Academic Press/Elsevier; 2011. 503-521 pp. DOI: 10.5688/ajpe77120

[33] Khan ZM, Law FCP, Adverse effects of pesticides and related chemicals on enzyme and hormone systems of fish, amphibians and reptiles: A review. *Proc Pakistan Acad Sci.* 2005;42:315-323.

[34] Lima Beluci NC, Affonso Pisano GM, Sayury Miyashiro C, Cândido Homem N, Guttierrez Gomesd R, Fagundes-Klenc MR, Bergamasco R, MarquetottiSalcedoVA. Hybrid treatment of coagulation/ flocculation process followed by ultrafiltration in TiO₂-modified membranes to improve the removal of reactive black 5 dye. *Sci. Total Environ.* 2019;664:222-229. DOI: 10.1016/j.scitotenv.2019.01.199

[35] Pradhan SS, Konwar K, Ghosh TN, Mondal B, Sarkar SK, Deb P, Multifunctional Iron oxide embedded reduced graphene oxide as a versatile adsorbent candidate for effectual arsenic and dye removal. *Colloid Interface Commun.* 2020;39: 100319. DOI; 10.1016/j.colcom.2020.100319

[36] Alvi MA, Shaheer Akhtar M, Effective photocatalytic dye degradation using low temperature grown zinc oxide nanostructures. *Mater. Letters.* 2020;281: 128609. DOI: 10.1016/j.matlet.2020.128609

[37] Mehta R, Brahmabhatt H, Mukherjee M, Bhattacharya A, Tuning separation behavior of tailor-made thin film poly(piperazine-amide) composite membranes for pesticides and salts from water. *Desalination.* 2017 ;404: 280-290. DOI: 10.1016/j.desal.2016.11.021

[38] Mohammadi P, Sheibani H, Evaluation, of the bimetallic photocatalytic performance of Resin–Au–Pd nanocomposite for degradation of parathion pesticide under visible

light. *Polyhedron.* 2019;170: 132-137. DOI: 10.1016/j.poly.2019.05.030

[39] Roca Jalil ME, Vieira R, Azevedo D, Baschini M, Sapag K, Improvement in the adsorption of thiabendazole by using aluminum pillared clays. *Appl. Clay Sci.* 2013;71: 55-63. DOI: 10.1016/j.clay.2012.11.005

[40] Romero-Pérez A, Infantes-Molina A, Jiménez-Lopez A, Jalil ER, Sapag K, Rodriguez-Castellon E, Al-pillared montmorillonite as a support for catalysts based on ruthenium sulfide in HDS reactions. *Catal. Today.* 2012;187: 88-96. DOI: 10.1016/j.cattod.2011.12.020

[41] Steudel A, Batenburg LF, Fischer HR, Weidler PG, Emmerich K, Alteration of non-swelling clay minerals and magadiite by acid activation. *Appl. Clay Sci.* 2009; 44: 95-104. DOI: 10.1016/j.clay.2009.02.001

[42] Eloussaief M, Benzina M, Efficiency of natural and acid-activated clays in the removal of Pb(II) from aqueous solutions. *J. Hazard. Mater.* 2010;178: 753-757. DOI: 10.1016/j.jhazmat.2010.02.004

[43] Medout-Marere V, Belarbi H, Thomas P, Morato F, Giuntini JC, Douillard JM, Thermodynamic analysis of the immersion of a swelling clay. *J. Colloid Interface Sci.* 1998; 202: 139-148. DOI: 10.1006/jcis.1998.5400

[44] Navia R. Environmental use of volcanic soil as natural adsorption material [PhD Thesis]. University of Leoben (Austria); 2004.

[45] Eren E, Afsin B, Onal Y, Removal of lead ions by acid activated and manganeseoxide-coated bentonite. *J. Hazard. Mater.* 2009;161:677-685. DOI: 10.1016/j.jhazmat.2008.04.020

[46] Thomas SM, Bertrand JA, Occelli ML, Huggins F, Gould SA, Microporous Montmorillonites Expanded

with Alumina Clusters and $M[(\mu\text{-OH})\text{Cu}(\mu\text{-OCH}_2\text{CH}_2\text{NEt}_2)]_6(\text{ClO}_4)_3$, ($M = \text{Al, Ga, and Fe}$), or $\text{Cr}[(\mu\text{-OCH}_3)(\mu\text{-OCH}_2\text{CH}_2\text{NEt}_2)\text{CuCl}]_3$ Complexes. *Inorg. Chem.* 1999;38(9): 2098-2105. DOI: 10.1021/ic981127g

[47] Tomić ZP, Logar VP, Babic BM, Rogan JR, Makreski P, Comparison of structural, textural and thermal characteristics of pure and acid treated bentonites from Aleksinac and Petrovac (Serbia). *Spectrochimica Acta Part A* 2011;82: 389-395. DOI: 10.1016/j.saa.2011.07.068

[48] Caglar B, Afsin B, Koksall E, Tabak A, Eren E, Characterization of Unye bentonite after treatment with sulfuric acid. *Quim. Nova.* 2013; 36: 955-959. DOI: 10.1590/S0100-40422013000700006

[49] Bhattacharyya KG, Gupta SS,. Adsorption of a few heavy metals on natural and modified kaolinite and montmorillonite: A review. *Adv. Colloid Interface Sci.* 2008;140: 114-131. DOI: 10.1016/j.cis.2007.12.008

[50] Giles CH, MacEwan TH, Nakhwa SN, Smith D, Studies in adsorption. Part XI: A system of classification of solution adsorption isotherms, and its use in diagnosis of adsorption mechanisms and in measurements of specific surface areas of solids. *J. Chem. Soc.* 1960;10: 3963-3973.

[51] Ho YS, Citation review of Langergren kinetic rate equation on adsorption reactions. *Scientometrics.* 2004;59 : 171-177. DOI: 10.1023/B:SCIE.0000013305.99473.cf

[52] Ho YS, McKay G, The kinetics of sorption of divalent metal ions onto sphagnum moss peat. *Water Res.* 2000;34: 735-742. DOI: 10.1016/S0043-1354(99)00232-8

[53] Komadel P, Chemically modified smectites. *Clay Miner.* 2003;38: 127-138. DOI: 10.1180/0009855033810083

[54] Fan QH, Shao DD, Hu J, Wu WS, Wang XK, Comparison of Ni^{2+} sorption to bare and ACT-graftattapulites: effect of pH, temperature and foreign ions. *Surf. Sci.* 2008;602: 778-785. DOI: 10.1016/j.susc.2007.12.007

[55] Wang XK, Chen CL, Hu WP, Ding AP, Xu D, Zhou X, Sorption of $^{243}\text{Am}(\text{III})$ to multiwall carbon nanotubes. *Environ. Sci. Technol.* 2005;39: 2856-2860. DOI: 10.1021/es048287d